

A general theory of inhomogeneous broadening for nonlinear susceptibilities: the polarizability and hyperpolarizability

Robert J. Kruhlak, and Mark G. Kuzyk

Abstract—While nonlinear optical spectroscopy is becoming more commonly used to study the excited states of nonlinear-optical systems, a general theory of inhomogeneous broadening is rarely applied in lieu of either a simple Lorentzian or Gaussian model. In this work, we generalize all the important linear and second-order nonlinear susceptibility expressions obtained with sum-over state quantum calculations to include Gaussian and stretched Gaussian distributions of Lorentzians. We show that using the correct model to analyze experiments that probe a limited wavelength range can be critical and that this theory is better able to fit the subtle spectral features - such as the shoulder region of a resonance - when both models produce qualitatively similar responses.

I. INTRODUCTION

WHEN calculating the nonlinear-optical susceptibilities near resonance, it is important to account for damping to get a reasonable approximation to the dispersion of a real molecule. Clearly, neglect of damping is catastrophic since sum-over-states (SOS) theories predict an infinite susceptibility on resonance. The SOS expression, as derived by Orr and Ward,[1] naturally admit damping corrections by making the eigenenergies of the system complex. The imaginary part of the energy is related to the resonance width and is called the natural linewidth. A stationary isolated molecule's line-shape is thus described by a Lorentzian. When the width is related to the intrinsic properties of a molecule, the width of a peak for a collection of noninteracting molecules is referred to as homogeneous broadening, i.e. the observed spectrum is the same as that of a single molecules times the number of molecules.

If the molecules interact or are placed in an environment with random perturbations, the natural linewidth is smeared out, leading to what is called inhomogeneous broadening (IB). Stoneham described in a detailed review article how the linear absorption spectrum in a crystal could be accurately modeled by applying stochastic averaging to a distribution of Lorentzians.[2] Since such statistical processes often lead to gaussian peak shapes such as the Boltzmann velocity distribution, systems with resonance features whose widths are much larger than the natural line width are often modeled by Gaussian functions.

Robert J. Kruhlak is at the Department of Physics, University of Auckland, Auckland, NZ E-mail: r.kruhlak@auckland.ac.nz

Mark G. Kuzyk is at the Department of Physics, Washington State University Pullman, Washington 99164-2814 E-mail: kuz@wsu.edu

Dirk et al[3] and Berkovic et al[4] showed that it was important to take damping into account by using a complex energy in the Orr and Ward SOS expression even when considering off-resonance susceptibilities. The distribution of molecules, when embedded in a polymer, are randomly perturbed by virtue of the fact that each molecule experiences a different local environment due to microscopic inhomogeneities. The distribution of sites around a molecule in a polymer can be measured[5], [6] and quantified by a stretched exponential distribution function.

Many excited states are often needed to correctly describe the dispersion of the hyperpolarizability[7], [8] and vibronic overtones may complicate the analysis.[9], [10] Since it has been shown that vibronic states are unimportant off-resonance,[11], [12] and on-resonance, we assume that their affect is smeared out due to thermal broadening (i.e. thermal fluctuations and the distribution of sites cause variations that are larger than vibronic energies), we argue that neglect of vibronic states and applying a stochastic averaging over Lorentzian functions using a stretched exponential weighting distribution function leads to a good model of the nonlinear spectra.

In this work, we focus on using the SOS expression to calculate the linear and second-order nonlinear-optical response under inhomogeneous broadening using the above approximations. (We will apply the same approach to the dipole-free SOS expression[13] in a future publication.) Our theoretical results are compared with experimental data in dye doped polymers for validation.

II. THEORY

Sum-over states quantum perturbation treatments of the b^{th} -order nonlinear susceptibility tensor, $\xi_{ij\dots k}^{(b)}$, in the dipole approximation yields a sum of terms of the form:[1]

$$\xi_{ij\dots k}^{(b)} \propto \sum_n \sum_m \dots \sum_l \frac{(\mu_i)_{gn} (\mu_j)_{nm} \dots (\mu_k)_{lg}}{(\omega_{ng} - i\Gamma_{ng} - \omega_1)(\omega_{mg} - i\Gamma_{mg} - \omega_1 - \omega_2)\dots}, \quad (1)$$

where $(\mu_i)_{nm}$ is the nm -matrix element of the i^{th} component of the electric dipole operator, ω_{nm} the transition frequency (energy) between states n and m , ω_i the frequency of the i^{th} optical field, and Γ_{ng} the phenomenological damping factor. The numerator is a product of $b + 1$ transition moments and the denominator a product of b energy terms. For an isolated

molecule, the damping factor Γ_{ng} is inversely proportional to the lifetime of state n and is a measure of the width of the peak in the spectrum of $\xi_{ij\dots k}^{(b)}$ associated with a transition between state n and the ground state g .

In real systems, molecules interact with each other yielding a broadening of the peaks in a spectrum. One common method to treat this case is to adjust the parameters Γ_{ng} . If the statistics of the molecules are Gaussian (as one finds in Doppler broadening), the Lorentzian function resulting from adjusting Γ_{ng} has the correct width but does not have a Gaussian shape. Another common method for modeling a nonlinear spectrum is to assume the peaks are Gaussian in shape. Depending on the region of interest (i.e near the peak or in the tail of the spectrum) one model may be more applicable than the other.

An exact method of treating inhomogeneous broadening is to apply the statistics of the molecular interactions to the susceptibility. Each molecule in an ensemble is then viewed as having a different transition frequency (energy), ω_{ng} . For example, if the statistics are Gaussian with a probability distribution of the form

$$f_{ng}(\delta\omega_{ng}) = \frac{1}{N(\gamma_{ng})} \exp \left[- \left(\frac{\delta\omega_{ng}}{\gamma_{ng}} \right)^2 \right], \quad (2)$$

where $\delta\omega_{ng} = \omega_{ng} - \bar{\omega}_{ng}$, $\bar{\omega}_{ng}$ is the mean value of the transition frequency, $N(\gamma_{ng})$ the normalization factor, and γ_{ng} the linewidth of the distribution - the susceptibility will be of the form,

$$\left(\int_{-\bar{\omega}_{ng}}^{\infty} d(\delta\omega_{ng}) \int_{-\bar{\omega}_{mg}}^{\infty} d(\delta\omega_{mg}) \dots \right) \xi_{ij\dots k}^{(b)}(\omega_{ng}, \omega_{mg}, \dots) f_{ng}(\delta\omega_{ng}) f_{mg}(\delta\omega_{mg}) \dots \quad (3)$$

Toussaere developed such a theory for second harmonic generation (SHG) and the Pockels effect using Gaussian statistics.[14]

In materials such as dye-doped polymers, the statistics that best model the effect of the distribution of sites on processes such as relaxation of molecular orientation order (which is normally an exponential process as described by Debye) is a stretched exponential. Using this analogy, we propose that variations in the local electric fields in a polymer yields the same statistics for modeling the susceptibility, so the distribution is also assumed to be a stretched Gaussian of the form,

$$f_{ng}(\delta\omega_{ng}) = \frac{1}{N(\gamma_{ng}, \beta)} \exp \left[- \left(\frac{\delta\omega_{ng}}{\gamma_{ng}} \right)^{2\beta} \right], \quad (4)$$

where β is the distribution of sites parameter, and for many systems - such as in dye-doped polymers - varies from $\beta = 0$ for an infinitely broad distribution to $\beta = 1$ for a single characteristic width. Again, $N(\gamma, \beta)$ is a normalization factor, which depends also on β , and will be written as

$$N(\gamma_{ng}, \beta) = \gamma_{ng} \sqrt{\pi} B(\beta), \quad (5)$$

where,

$$B(\beta) = \left[\frac{1}{\gamma_{ng} \sqrt{\pi}} \int_{-\infty}^{\infty} \exp \left[- \left(\frac{\delta\omega_{ng}}{\gamma_{ng}} \right)^{2\beta} \right] d(\delta\omega_{ng}) \right] \quad (6)$$

to remain compatible with previous inhomogeneous broadening representations which use Gaussian statistics [14], [15], [16], [17]. Indeed, such statistics other than pure Gaussian were observed in light scattering experiments [18], [16], [17].

A. Normalization and Approximations

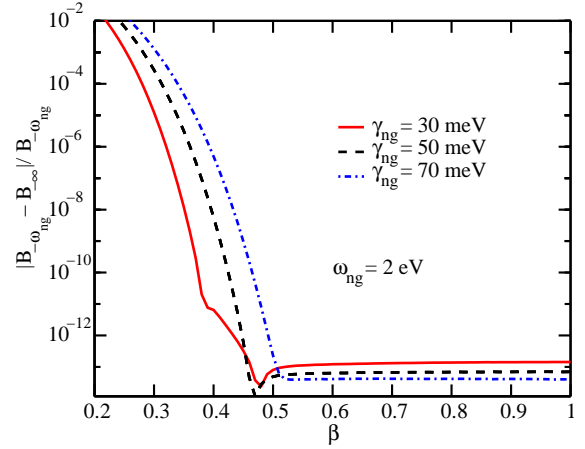


Fig. 1. Relative difference between $B(\beta)$ when the integral is taken over all frequency space, and when the lower limit for $B(\beta)$ is given by $\omega_{ng} = 2$ eV

Because $B(\beta)$ is difficult to calculate, we need to make simplifying assumptions. Typical inhomogeneous linewidths are narrow compared with the transition frequency [19], [17], so we can integrate over all space even though there is a finite lower limit to the integral. Furthermore, we assume that $B(\beta)$ is independent of γ_{ng} . Figure 1 shows the relative difference between $B(\beta)$ determined by integrating of over all frequency space and integration to a lower limit of $\omega_{ng} = 2$ eV. Clearly, if the inhomogeneous linewidth is smaller than 70 meV – which is the case for all our experimental data – this assumption leads to a negligible relative difference ($< 1\%$) for $\beta > 0.3$.

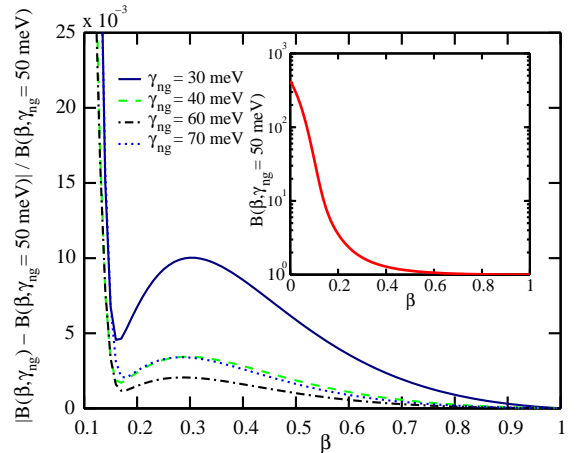


Fig. 2. Relative difference between $B(\beta, \gamma_{ng})$ and $B(\beta, \gamma_{ng} = 50$ meV)

The second assumption is that the normalization function $B(\beta)$ is independent of the inhomogeneous linewidth, γ_{ng} .

Figure 2 shows that this assumption is valid to good approximation (within 1%) for $\beta > 0.15$ (see inset in Figure 2). The reference value of $B(\beta, \gamma_{ng} = 50 \text{ meV})$ was chosen because it is a typical linewidth for the chromophores we consider. These assumptions allow us to calculate one normalization function independent of ω_{ng} and γ_{ng} when we consider $\beta > 0.3$, which is critical for decreasing the computation time of the theory when applied to a least-squares fit to the data.

In this paper, we derive the expressions for the most important linear and second-order susceptibilities for any general statistics. Specific results are presented for Gaussian and stretched exponential susceptibilities that model the SHG response (hyperpolarizability) for a two-level system and data from linear absorption experiments (polarizability) on silicon phthalocyanine-(mono)methylmethacrylate(SiPc) doped (poly)methylmethacrylate (PMMA) thin films. All the expressions for the second-order processes are displayed in detail in Appendix B.

B. First-Order Susceptibility

In this section, we outline the approach of the calculation for a general distribution function for a linear susceptibility (which has one energy denominator) and in the next section apply the theory to a second-order susceptibility (which has two energy denominators). These two cases can be easily generalized to any-order susceptibility and any statistics.

From time dependent perturbation theory, the 1-D first-order molecular susceptibility is [20], [19]:

$$\xi^{(1)}(-\omega; \omega) = \frac{1}{\epsilon_0! \hbar} \sum_n \{ \mu_{gn} \mu_{ng} D_n^L(-\omega; \omega) \}, \quad (7)$$

where

$$D_n^L(-\omega; \omega) = \left\{ \frac{1}{\Omega_{ng} - \omega} + \frac{1}{\Omega_{ng}^* + \omega} \right\}. \quad (8)$$

The inhomogeneous broadened Lorentzian function is then

$$D_n^{IB}(-\omega; \omega) = \int_{-\omega_{ng}}^{\infty} D_n^L(-\omega; \omega) f_{ng}(\delta\omega_{ng}) d(\delta\omega_{ng}). \quad (9)$$

Once $D_n^{IB}(-\omega; \omega)$ is known it can be substituted into Eq. (7) for $D_n^L(-\omega; \omega)$ to create an inhomogeneously broadened microscopic susceptibility. To this end, we proceed to determine the first term in Equation (9). Substituting Equation (4) for the Gaussian function, changing the integration variable to $t = (\omega'_{ng} - \omega_{ng})/\gamma_{ng}$, and rearranging the denominator so that $z = (-\omega_{ng} + i\Gamma_{ng} + \omega)/\gamma_{ng}$ gives the following

$$\begin{aligned} & \int_{-\omega_{ng}}^{\infty} \frac{1}{\omega'_{ng} - i\Gamma_{ng} - \omega} f_{ng}(\omega'_{ng} - \omega_{ng}) d(\omega'_{ng} - \omega_{ng}) \\ &= \frac{1}{\gamma_{ng} \sqrt{\pi} B(\beta)} \int_{-\frac{\omega_{ng}}{\gamma_{ng}}}^{\infty} \frac{\exp(-t^{2\beta})}{t + (\frac{\omega_{ng} - i\Gamma_{ng} - \omega}{\gamma_{ng}})} dt, \\ &\simeq -\frac{1}{\gamma_{ng} \sqrt{\pi} B(\beta)} \int_{-\infty}^{\infty} \frac{\exp(-t^{2\beta})}{z - t} dt. \end{aligned} \quad (10)$$

To simplify the expression in Equation (10), we define $W_\beta^{(k)}(z)$ as the following:

$$W_\beta^{(k)}(z) = \frac{i}{\pi B(\beta)} \int_{-\frac{\omega_{ng}}{\gamma_{ng}}}^{\infty} \frac{\exp(-t^{2\beta})}{(z - t)^k} dt, \quad (11)$$

and the complex error function as [21],

$$W(z) = \frac{i}{\pi} \int_{-\infty}^{\infty} \frac{\exp(-t^2)}{z - t} dt \quad (12)$$

The second term in Eq. (9) is derived analogously so we write the first-order energy denominator that accounts for inhomogeneous broadening as:

$$D_n^{IB}(-\omega; \omega) = \frac{i\sqrt{\pi}}{\gamma_{ng}} \times \left[W_\beta^{(1)} \left(\frac{-(\Omega_{ng} - \omega)}{\gamma_{ng}} \right) + W_\beta^{(1)} \left(\frac{-(\Omega_{ng}^* + \omega)}{\gamma_{ng}} \right) \right]. \quad (13)$$

In the limit that $\beta = 1$, the first-order energy denominator can be written in terms of the complex error function, $W(z)$ [14], [15], [16]:

$$D_n^{IB}(-\omega; \omega) = \frac{i\sqrt{\pi}}{\gamma_{ng}} \times \left[W \left(\frac{-(\Omega_{ng} - \omega)}{\gamma_{ng}} \right) + W \left(\frac{-(\Omega_{ng}^* + \omega)}{\gamma_{ng}} \right) \right], \quad (14)$$

which can be evaluated for all values of z using the results in Abramowitz and Stegun [21]. The general transformation from the Lorentzian model to the inhomogeneous broadening model is summarized in Table III.

C. Second-Order

Using time dependent perturbation theory, we define a second-order Lorentzian energy denominator as:

$$D_{lm}^L(-\omega_\sigma; \omega_1, \omega_2) = \mathbf{S}_{1,2} \left\{ [(\Omega_{lg} - \omega_\sigma)(\Omega_{mg} - \omega_1)]^{-1} + [(\Omega_{lg}^* + \omega_2)(\Omega_{mg} + \omega_\sigma)]^{-1} + [(\Omega_{lg}^* + \omega_2)(\Omega_{mg} - \omega_1)]^{-1} \right\}, \quad (15)$$

where $\mathbf{S}_{1,2}$ is the permutation operator, which averages over all distinct permutations of ω_1 , and ω_2 .

It is significantly more difficult to transform nonlinear Lorentzian energy denominators to nonlinear IB energy denominators because of the product of Lorentzian terms in the denominator. In order to transform D_{lm}^L for a specific experiment (i.e. for specific input and output frequencies), the number of excited states must be known prior to performing a partial fraction expansion on each term in the energy denominators. For example if there is only one distinct excited state (l), it may be necessary to perform the following partial fraction expansion,

$$\frac{1}{(\Omega_{lg} - \omega)\Omega_{lg}} = \frac{1}{\omega} \left[\frac{1}{(\Omega_{lg} - \omega)} - \frac{1}{\Omega_{lg}} \right], \quad (16)$$

to eliminate the product of the two Ω_{lg} terms. These type of expansions allow us to write the nonlinear energy denominators in terms of $W_\beta^{(1)}(z)$ or complex error functions.

However, a perfect square in the denominator requires a different approach. The approach for evaluating the fundamental transformations from the homogeneous formulation to the inhomogeneous formulation for the quadratic dependencies (cubic dependencies are studied in Ref. [22]) on the transition frequency, ω_{lg} is shown below.

Beginning with a quadratically dependent term like the following,

$$\frac{C_2}{(\omega'_{ng} - i\Gamma_{ng} - \omega)^2} \quad (17)$$

we integrate its product with the distribution function (Equation (4)),

$$\int_{-\omega_{ng}}^{\infty} \frac{C_2}{(\omega'_{ng} - i\Gamma_{ng} - \omega)^2} f_{ng}(\omega'_{ng} - \omega_{ng}) d(\omega'_{ng} - \omega_{ng}), \quad (18)$$

as the initial step in the transform. Substituting Equation (4) for $f_{ng}(\omega'_{ng} - \omega_{ng})$, and changing the integration variable to $t = (\omega'_{ng} - \omega_{ng})/\gamma_{ng}$, results in the following:

$$\begin{aligned} & \int_{-\omega_{ng}}^{\infty} \frac{C_2}{(\omega'_{ng} - i\Gamma_{ng} - \omega)^2} f_{ng}(\omega'_{ng} - \omega_{ng}) d(\omega'_{ng} - \omega_{ng}) \\ &= \frac{C_2}{\gamma_{ng} \sqrt{\pi} B(\beta)} \int_{-\omega_{ng}}^{\infty} \frac{\exp(-(\frac{\omega'_{ng} - \omega_{ng}}{\gamma_{ng}})^{2\beta})}{(\omega'_{ng} - i\Gamma_{ng} - \omega)^2} d(\omega'_{ng} - \omega_{ng}), \\ &= \frac{C_2}{\gamma_{ng} \sqrt{\pi} B(\beta)} \int_{-\frac{\omega_{ng}}{\gamma_{ng}}}^{\infty} \frac{\gamma_{ng} \exp(-t^{2\beta})}{(\omega'_{ng} - i\Gamma_{ng} - \omega)^2} dt, \\ &= \frac{C_2}{\gamma_{ng} \sqrt{\pi} B(\beta)} \int_{-\frac{\omega_{ng}}{\gamma_{ng}}}^{\infty} \frac{\gamma_{ng} \exp(-t^{2\beta})}{(\omega_{ng} + \gamma_{ng}t - i\Gamma_{ng} - \omega)^2} dt, \\ &= \frac{C_2}{\gamma_{ng} \sqrt{\pi} B(\beta)} \int_{-\frac{\omega_{ng}}{\gamma_{ng}}}^{\infty} \frac{\gamma_{ng} \exp(-t^{2\beta})}{\gamma_{ng}^2 (t + \frac{\omega_{ng} - i\Gamma_{ng} - \omega}{\gamma_{ng}})^2} dt, \\ &= \frac{C_2}{\gamma_{ng}^2 \sqrt{\pi} B(\beta)} \int_{-\frac{\omega_{ng}}{\gamma_{ng}}}^{\infty} \frac{\exp(-t^{2\beta})}{(z - t)^2} dt, \\ &= \frac{C_2 i \sqrt{\pi}}{\gamma_{ng}} \left[\frac{-1}{\gamma_{ng}} W_{\beta}^{(2)}(z) \right] \end{aligned} \quad (19)$$

where $z = (-\omega_{ng} + i\Gamma_{ng} + \omega)/\gamma_{ng}$. In the limit that $\beta = 1$, Equation (19) looks very similar to Equation (10) just before substituting for $W(z)$ except that the denominator in the integral is second-order in $(z - t)$. To reduce the denominator to first-order in $(z - t)$ so that the integral can be replaced with $W(z)$, we perform integration by parts twice:

$$\begin{aligned} \int_{-\frac{\omega_{ng}}{\gamma_{ng}}}^{\infty} \frac{T}{(z - t)^2} dt &= \frac{T}{z} \Big|_{t=-\frac{\omega_{ng}}{\gamma_{ng}}}^0 + \int_{-\frac{\omega_{ng}}{\gamma_{ng}}}^{\infty} \frac{2tT}{(z - t)^2} dt, \\ &= 2z \int_{-\frac{\omega_{ng}}{\gamma_{ng}}}^{\infty} \frac{T}{(z - t)^2} dt - 2 \int_{-\frac{\omega_{ng}}{\gamma_{ng}}}^{\infty} T dt, \\ &\simeq -2i\pi z W(z) - 2\sqrt{\pi}, \end{aligned} \quad (20)$$

where we have used $T = \exp(-t^2)$ to simplify the presentation. The first term on the right on the top line of Equation (20) vanishes because the argument of the exponential is $\approx -10^3$ at the lower limit (usually $\omega \gg \gamma$ in the visible). Note that Equation (20) is kept general (the lower limit of integration is not approximated as $-\infty$). We only use this approximation as needed for special cases. To get the second line of Equation (20), we use $t/(z - t) = z/(z - t) - 1$. Therefore we can write

Equation (18), when $\beta = 1$, as the following,

$$\begin{aligned} & \int_{-\omega_{ng}}^{\infty} \frac{C_2}{(\omega'_{ng} - i\Gamma_{ng} - \omega)^2} f_{ng}(\omega'_{ng} - \omega_{ng}) d(\omega'_{ng} - \omega_{ng}) \\ &= \frac{C_2}{\gamma_{ng}^2 \sqrt{\pi}} \{-2i\pi z W(z) - 2\sqrt{\pi}\} \\ &= \frac{C_2 i \sqrt{\pi}}{\gamma_{ng}} \left\{ \frac{-2z}{\gamma_{ng}} W(z) + \frac{2i}{\sqrt{\pi} \gamma_{ng}} \right\}. \end{aligned} \quad (21)$$

Thus we have derived the convolution of a second-order denominator term with a Gaussian, which can be generalized to any complex term that has a second-order dependence on $(z - t)$.

Table III in Appendix A summarizes the fundamental energy denominators up to second-order for the Lorentzian and IB theories with $\beta \leq 1$, and $\beta = 1$, respectively. These two transformations can be used to construct any IB energy denominator for any first-, and/or second-order response.

TABLE I
COMPACT FORM OF $W_{\beta}^{(x)}(z)$ AND $W(z)$.

β	Term	Compact Form
≤ 1	$W_{\beta}^{(x)} \left(\frac{-(\Omega_{ng} \mp \omega_i)}{\gamma_{ng}} \right)$	$W_{\beta_n}^{(x)}(\mp \omega_i)$
	$W_{\beta}^{(x)*} \left(\frac{-(\Omega_{ng}^* \pm \omega_i)}{\gamma_{ng}} \right)$	$W_{\beta_n}^{(x)*}(\pm \omega_i)$
1	$W \left(\frac{-(\Omega_{lg} \mp \omega_i)}{\gamma_{lg}} \right)$	$W_l(\mp \omega_i)$
	$W \left(\frac{-(\Omega_{lg}^* \pm \omega_i)}{\gamma_{lg}} \right)$	$W_l^*(\pm \omega_i)$

The energy denominators $D_{lm\dots}$ for the second-(and higher)-order susceptibilities are complex combinations of $W_{\beta}^{(x)}(z)$ or $W(z)$. To make them more readable we have developed a compact notation. For $\beta \leq 1$, we have added a subscript to β to indicate the excited state involved in the process and a * on the power of W to indicate a complex conjugate of the complex argument $\Omega_{ng} = \omega_{ng} - i\Gamma_{ng}$. Similarly for $\beta = 1$, the subscript on W indicates the excited state and the superscript * on W indicates the complex conjugate of Ω . This allows us to use a simple frequency argument of $\pm\omega$ which significantly improves the readability of the equations in Appendix B. An example of the transformation to the compact notation is given below:

$$W_{\beta}^{(1)} \left(\frac{-(\Omega_{2g}^* + \omega_3)}{\gamma_{2g}} \right) \rightarrow W_{\beta_2}^{(1)*}(\omega_3) \quad (22)$$

This compact form is sufficient to describe all of the inhomogeneous broadening contributions to the energy denominators in this paper because the arguments are all of the form $\frac{-(\Omega_{ng}^* \pm \omega_i)}{\gamma_{ng}}$ or $\frac{-(\Omega_{ng} \mp \omega_i)}{\gamma_{ng}}$ and all of the excited state transitions are from/to the ground state (g). Table I summarizes the transformations to the compact notation.

D. Linear Susceptibility

In this section we discuss the effects of β on the linear response of a dye-doped polymer system with one excited state. Figure 3 shows the real and imaginary parts of the linear

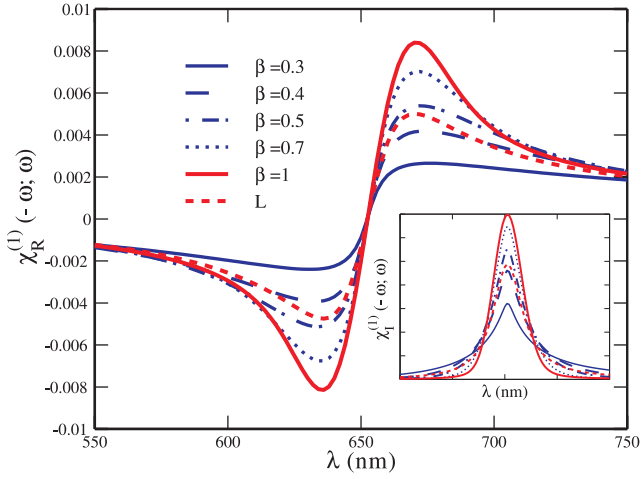


Fig. 3. Real and imaginary [inset] parts of $\chi^{(1)}(-\omega; \omega)$ for a single excited state centered at 653 nm for various values of β . For all values of β , $\Gamma = 10$ meV and $\gamma = 50$ meV. The homogeneous-broadening (Lorentzian) theory of the electronic transition is denoted by L and $\Gamma = 50$ meV.

susceptibility, which is proportional to Eq. (7) with $n = 1$ and the appropriate energy denominators, for various values of β in the IB model. For comparison the homogeneous (Lorentzian) theory is denoted by L. We use typical values for the transition moment and homogeneous and inhomogeneous linewidths. In this example the excited state is centered at about 653 nm with a transition moment of 11.5 D. For all the IB curves the Lorentzian linewidth is 10 meV, and the IB linewidth is 50 meV. The Lorentzian curve is generated using a 50 meV linewidth and the same center frequency and transition moment as the IB curves. As we expect the magnitude of the response for a fixed inhomogeneous linewidth decreases and becomes broader as the distribution of sites within the polymer matrix increases (decreasing β). To better describe the effects

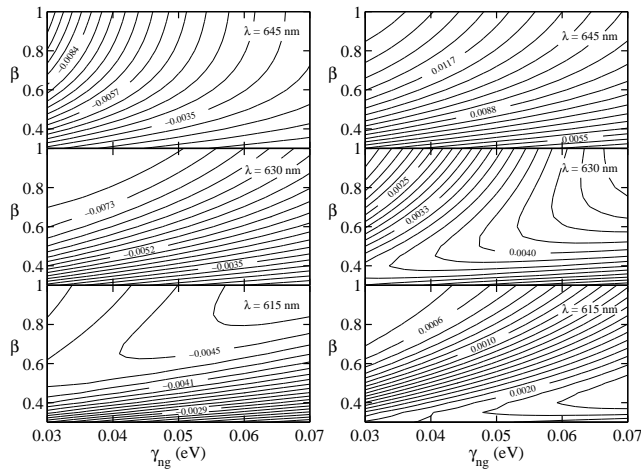


Fig. 4. Contours of the real (left) and imaginary (right) parts of $\chi^{(1)}(-\omega; \omega)$ generated using the generalized IB theory for a single excited state centered at 653 nm ($\mu_{ng} = 11.5$ D, $\Gamma_{ng} = 10$ meV) for three probe wavelengths (615 nm, 630 nm, 645 nm).

of the distribution of sites, IB, and homogenous broadening in the linear response we plot the real and imaginary parts

of $\chi^{(1)}(-\omega; \omega)$ as a function of β (distribution of sites) and γ_{ng} (IB) for fixed Γ_{ng} (L) and $\chi^{(1)}(-\omega; \omega)$ as a function of β and Γ_{ng} for fixed γ_{ng} . In Figure 4, the single excited state transition is centered at 653 nm, with a transition dipole moment of 11.5 D, and a fixed Lorentzian linewidth of 10 meV, while Figure 5 uses a fixed IB linewidth, γ_{ng} of 50 meV.

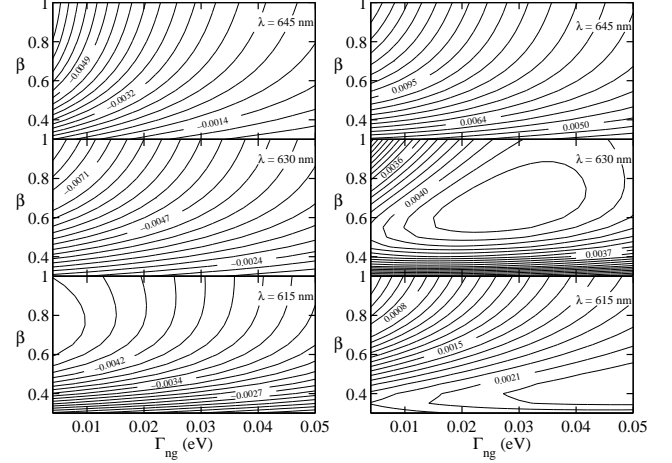


Fig. 5. Contours of the real and imaginary parts of $\chi^{(1)}(-\omega; \omega)$ generated using the generalized IB theory for a single excited state centered at 653 nm ($\mu_{ng} = 11.5$ D, $\gamma_{ng} = 50$ meV) for three probe wavelengths (615 nm, 630 nm, 645 nm).

Figures 4 and 5 each show a distinct character of $\chi^{(1)}(-\omega; \omega)$ for wavelengths between 615 nm and 645 nm. The β parameter therefore gives an additional degree of freedom for modeling guest/host materials where a distribution of sites requires using non-Gaussian statistics for both the index of refraction and the absorption coefficient.

III. SECOND-ORDER SUSCEPTIBILITY

In this section, we demonstrate that there are significant differences in the response from two-level systems depending on the broadening model. We concentrate on second harmonic generation (SHG) as an example because of its near-universal use in characterizing molecules. For a two-level system, the SHG hyperpolarizability $\chi^{(2)}(-2\omega; \omega, \omega) \propto D_{ll}(-2\omega; \omega, \omega)$ [see Eq (23) and Eq. (25) for the IB models, and Eq. (15) for the L model] where l in this case is 1.

TABLE II
INHOMOGENEOUS AND LORENTZIAN BROADENING PARAMETERS FOR A TWO-LEVEL SYSTEM.

Model	ω_{1g}	Γ_{1g}	γ_{1g}
L	1.85 eV	0.05 eV	-
IB	1.85 eV	0.025 eV	0.05 eV

Figure 6 shows the response of a two-level system using the parameters in Table II. For the IB model four values of β have been studied as shown in the legend. It is clear that the response in the IR for all models are qualitatively similar but quantitatively different. Thus a fit to an SHG experiment that

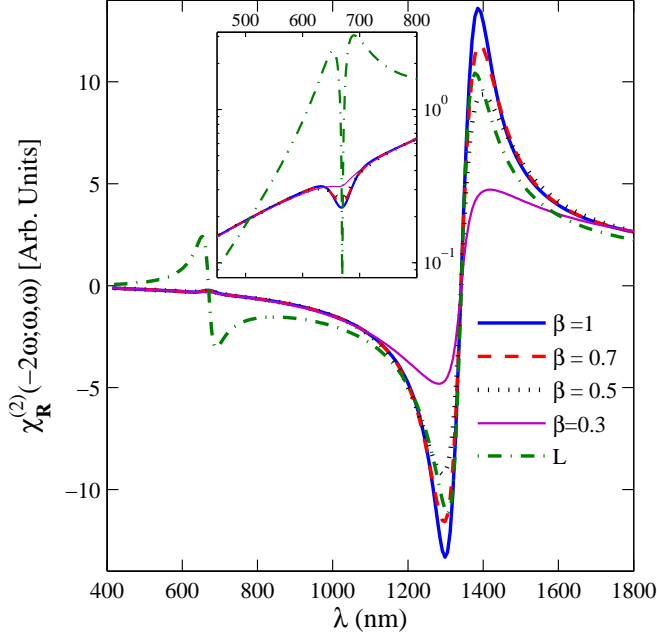


Fig. 6. Second harmonic generation response for several inhomogeneously broadened two level systems. The real part of $\chi^{(2)}(-2\omega; \omega, \omega)$ is shown as a function of the incident wavelength. A homogeneously broadened (L) response is included for comparison. The inset shows the magnitude on a log scale in the visible region. Parameters for the curves can be found in Table II.

probes this system in the IR region would come to a similar conclusion for the parameters describing which excited states are involved in the process. The difference between the two models could be used to estimate the error.

In the visible part of the spectrum (see inset), the different models do not agree with each other, where the L model is dramatically different both qualitatively and quantitatively from the IB models. This becomes important for those experiments that probe the system over a limited wavelength range (or more egregiously, at a single wavelength) and attempt to determine an off-resonance value for the hyperpolarizability. In this example, an SHG experiment that probed this one-level system only in the visible would determine a completely different set of parameters depending on the model used to interpret the results.

IV. COMPARISON OF THEORY TO EXPERIMENTAL RESULTS

Next, we compare IB Lorentzian models with linear absorption data from (SiPc/PMMA) thin films[23] to show that the wing region of the linear absorption resonance is often better described using an inhomogeneous broadening model. A similar comparison for the quadratic electroabsorption spectrum of this molecule can be found in the literature.[23], [22]

Figure 7 compares SiPc experimental linear absorption data with the Lorentzian (L) theory, and the IB theory for two values of β . A least squares fit gives $\beta = 0.9$. It is possible that the high-energy side of the peak is affected by the next excited state, so a least squares fit was performed from the peak to

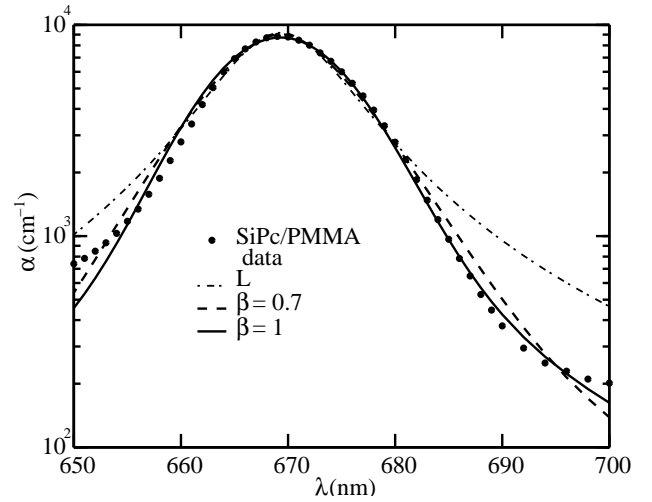


Fig. 7. Linear absorption of SiPc/PMMA in comparison to least-squares fits using Lorentzian and IB theories ($L = \{\mu_{1g} = 8 \text{ D}, \text{ and } \Gamma_{1g} = 18 \text{ meV}\}$, $IB(\beta = 1) = \{\mu_{1g} = 7.4 \text{ D}, \Gamma_{1g} = 9 \text{ meV}, \text{ and } \gamma_{1g} = 19 \text{ meV}\}$, $IB(\beta = 0.7) = \{\mu_{1g} = 7.5 \text{ D}, \Gamma_{1g} = 7 \text{ meV}, \text{ and } \gamma_{1g} = 18 \text{ meV}\}$).

the low-energy side. This gives a least squares fit of $\beta = 1$. In either case, it appears that the distribution of sites is narrow in the SiPc/PMMA system. The result is reasonable given that the SiPc molecule is non-dipolar so there are no dipole interactions with the surroundings. All broadening therefore results from higher-order multipoles, which contribute more weakly to the width.

Given that the calculated homogeneous broadened linewidths for each model compare well with the literature on the temperature dependence of these linewidths for doped PMMA systems,[24] it is clear that the IB model describes the response better than the Lorentzian model especially in the wings of the resonance. It should therefore give a better estimate of zero-frequency susceptibilities for comparison with the Thomas-Kuhn sum-rule quantum limit.[25], [26], [27], [28] Indeed, it would be interesting to apply inhomogeneous broadening models to the fundamental limits of the dispersion of the hyperpolarizability.[29] It may very well be the case that the gap between the best nonlinear-optical molecules and the fundamental limit[11], [12], [28] may be partially explained by inaccuracies in the dispersion model.

V. CONCLUSION

In conclusion, we calculate the inhomogeneously broadened linear and second-order nonlinear susceptibilities for a Gaussian and stretched Gaussian distribution of Lorentzians. A Lorentzian model is found to be inaccurate in predicting the shape of the linear absorption spectrum of SiPc/PMMA. However, the IB-broadened theory fits the data over a broad range of wavelengths and shows that the distribution of sites is nearly Gaussian, implying that interactions between the polymer and dopant are small, as we would expect of a non-dipolar molecule.

Since the nature of the broadening mechanisms, especially for nonlinear spectroscopy, is shown to affect the dispersion

dramatically, the determination of excited state properties of molecules from spectroscopy requires that such a theory be used. Indeed, the inconsistency of transition moments as determined by different processes (i.e. linear versus nonlinear spectroscopy) may be due in part to the use of inappropriate dispersion models. Furthermore, the practice of extrapolating single-wavelength measurements to get the off-resonance hyperpolarizability, β_0 , [30] may lead to large inaccuracies. As such, IB theory may be an important tool for interpreting any nonlinear-optical experiment.

ACKNOWLEDGMENTS

We thank the National Science Foundation (ECS-0354736) and Wright Patterson Air Force Base for generously supporting this work.

REFERENCES

- [1] B. J. Orr and J. F. Ward, "Perturbation Theory of the Non-Linear Optical Polarization of an Isolated System," *Molecular Physics* **20**, 513–526 (1971).
- [2] A. M. Stoneham, "Shapes of Inhomogeneously Broadened Resonance Lines in Solids," *Review of Modern Physics* **41**, 82–108 (1969).
- [3] C. W. Dirk and M. G. Kuzyk, "Damping Corrections and the Calculation of Optical Nonlinearities in Organic Molecules," *Phys. Rev. B* **41**, 1636–1639 (1990).
- [4] G. Berkovic, G. Meshulam, and Z. Kolter, "Measurement and analysis of molecular hyperpolarizability in the two-photon resonance regime," *J. Chem. Phys.* **112**, 3997–4003 (2000).
- [5] F. Ghebremichael and M. G. Kuzyk, "Optical Second-Harmonic Generation as a Probe of the Temperature Dependence of the Distribution of Sites in a Poly(methyl Methacrylate) Polymer Doped with Disperse Red 1 Azo Dye," *J. Appl. Phys.* **77**, 2896–2901 (1995).
- [6] F. Ghebremichael, M. G. Kuzyk, and H. Lackritz, "Nonlinear optics and polymer physics," *Prog. Polymer Sci.* **22**, 1147–1201 (1997).
- [7] C. W. Dirk and M. G. Kuzyk, "Missing-state analysis: A method for determining the origin of molecular nonlinear optical properties," *Phys. Rev. A* **39**, 1219–1226 (1989).
- [8] B. Champagne and B. Kirtman, "Evaluation of alternative sum-over-states expressions for the first hyperpolarizability of push-pull pi-conjugated systems," *J. Chem. Phys.* **125**, 024101 (2006).
- [9] C. H. Wang, "Effects of dephasing and vibronic structure on the first hyperpolarizability of strongly charge-transfer molecules," *J. Chem. Phys.* **112**, 1917–1924 (2000).
- [10] C. H. Wang, J. N. Woodford, C. Zhang, and L. R. Dalton, "Resonant and Nonresonant Hyper-Rayleigh Scattering of Charge-Transfer Chromophores," *J. Appl. Phys.* **89**, 4209–4217 (2001).
- [11] K. Tripathi, P. Moreno, M. G. Kuzyk, B. J. Coe, K. Clays, and A. M. Kelley, "Why hyperpolarizabilities Fall Short of the Fundamental Quantum Limits," *J. Chem. Phys.* **121**, 7932–7945 (2004).
- [12] K. Tripathy, J. Pérez Moreno, M. G. Kuzyk, B. J. Coe, K. Clays, and A. M. Kelley, "Erratum: Why Hyperpolarizabilities Fall Short of the Fundamental Quantum Limits," *J. Chem. Phys.* **125**, 079905 (2006).
- [13] M. G. Kuzyk, "Compact sum-over-states expression without dipolar terms for calculating nonlinear susceptibilities," *Phys. Rev. A* **72**, 053819 (2005).
- [14] E. Toussaere, *Polymer electrooptiques pour optique non lineaire caracterisation optique et modeles statistiques*, Ph.D. thesis, University of Paris (1993).
- [15] A. Otomo, *Second order optical nonlinearities and wave mixing devices in poled polymer waveguides*, Ph.D. thesis, University of Central Florida (1995).
- [16] R. J. Kruhlak and M. G. Kuzyk, "Side-Illumination Fluorescence Spectroscopy. I. Principles," *J. Opt. Soc. Am. B* **16**, 1749–1755 (1999).
- [17] R. J. Kruhlak and M. G. kuzyk, "Side-Illumination Fluorescence Spectroscopy. II. Applications to Squaraine-Dye-Doped Polymer Optical Fibers," *J. Opt. Soc. Am. B* **16**, 1756–1767 (1999).
- [18] R. J. Kruhlak, J. Young, and M. G. Kuzyk, "Loss and correlation measurements in squarinedoped nonlinear polymer optical fibers," *SPIE Proc.* **3147**, 11828 (1997).
- [19] R. J. Kruhlak, *Characterization of molecular excited states for nonlinear optics*, Ph.D. thesis, Washington State University (2000).
- [20] P. N. Butcher and D. Cotter, *The elements of nonlinear optics* (Cambridge University Press, Cambridge, 1990), 1st edn.
- [21] M. Abramowitz and I. E. Stegun, *Handbook of Mathematical Functions* (U. S. Government Printing Office, Washington, D. C., 1972).
- [22] R. J. Kruhlak and M. G. Kuzyk, "A general theory of inhomogeneous broadening for nonlinear susceptibilities: the second hyperpolarizability," *IEEE Journal on Selected Topics in Quantum Electronics* (2008).
- [23] R. J. Kruhlak and M. G. Kuzyk, "Measuring the electronic third-order susceptibility of the silicon-phthalocyanine-monomethacrylate molecule with quadratic electroabsorption spectroscopy," *J. Opt. Soc. Am. B* **22**, 643 (2005).
- [24] A. J. Garcia and J. Fernandez, "Optical homogeneous linewidths in glasses in the framework of the soft-potential model," *Phys. Rev. B* **56**, 579–592 (1997).
- [25] M. G. Kuzyk, "Physical Limits on Electronic Nonlinear Molecular Susceptibilities," *Phys. Rev. Lett.* **85**, 1218 (2000).
- [26] M. G. Kuzyk, "Fundamental limits on third-order molecular susceptibilities: erratum," *Opt. Lett.* **28**, 135 (2003).
- [27] M. G. Kuzyk, "Fundamental limits on third-order molecular susceptibilities," *Opt. Lett.* **25**, 1183 (2000).
- [28] M. G. Kuzyk, "Erratum: Physical Limits on Electronic Nonlinear Molecular Susceptibilities," *Phys. Rev. Lett.* **90**, 039902 (2003).
- [29] M. G. Kuzyk, "Fundamental limits of all nonlinear-optical phenomena that are representable by a second-order susceptibility," *J. Chem Phys.* **125**, 154108 (2006).
- [30] M. G. Kuzyk and C. W. Dirk, *Characterization techniques and tabulations for organic nonlinear optical materials* (Marcel Dekker, 1998).

APPENDIX A
ENERGY DENOMINATOR TRANSFORMATIONS

TABLE III
FUNDAMENTAL ENERGY (FREQUENCY) DIFFERENCE CONTRIBUTIONS TO HOMOGENEOUSLY BROADENED (L) AND INHOMOGENEOUSLY BROADENED (IB) ELECTRONIC TRANSITIONS UP TO SECOND-ORDER.

Lorentzian (L)	($\beta \leq 1$)	Inhomogeneous Broadening (IB)	($\beta = 1$)
$\frac{C_1}{\omega_{ng} \mp i\Gamma_{ng} \mp \omega}$	$\frac{i\sqrt{\pi}C_1}{\gamma_{ng}} W_{\beta}^{(1)} \left(\frac{-\omega_{ng} \pm i\Gamma_{ng} \pm \omega}{\gamma_{ng}} \right)$	$\frac{i\sqrt{\pi}C_1}{\gamma_{ng}} W \left(\frac{-\omega_{ng} \pm i\Gamma_{ng} \pm \omega}{\gamma_{ng}} \right)$	
$\frac{C_2}{(\omega_{ng} \mp i\Gamma_{ng} \mp \omega)^2}$	$\frac{i\sqrt{\pi}C_2}{\gamma_{ng}} \left[\frac{-1}{\gamma_{ng}} W_{\beta}^{(2)} \left(\frac{-\omega_{ng} \pm i\Gamma_{ng} \pm \omega}{\gamma_{ng}} \right) \right]$	$\frac{i\sqrt{\pi}C_2}{\gamma_{ng}} \left\{ \frac{2(\omega_{ng} \mp i\Gamma_{ng} \mp \omega)}{\gamma_{ng}^2} W \left(\frac{-\omega_{ng} \pm i\Gamma_{ng} \pm \omega}{\gamma_{ng}} \right) + \frac{2i}{\sqrt{\pi}\gamma_{ng}} \right\}$	

APPENDIX B
ENERGY DENOMINATORS FOR SECOND-ORDER PROCESSES

A. Second-Harmonic Generation

1) $\beta \leq 1$:

$$D_{ll}^{IB}(-2\omega; \omega, \omega) = \frac{i\sqrt{\pi}}{\gamma_{lg}} \times \left\{ \frac{1}{\omega} \left[W_{\beta_l}^{(1)}(-2\omega) - W_{\beta_l}^{(1)}(-\omega) + W_{\beta_l}^{(1)*}(\omega) - W_{\beta_l}^{(1)*}(2\omega) \right] + \frac{1}{2(\omega + i\Gamma_{lg})} \left[W_{\beta_l}^{(1)}(-\omega) - W_{\beta_l}^{(1)*}(\omega) \right] \right\} \quad (23)$$

$$D_{lm}^{IB}(-2\omega; \omega, \omega) = \frac{-\pi}{\gamma_{lg}\gamma_{mg}} \left\{ W_{\beta_l}^{(1)}(-2\omega)W_{\beta_m}^{(1)}(-\omega) + W_{\beta_l}^{(1)*}(\omega) \left[W_{\beta_m}^{(1)*}(2\omega) + W_{\beta_m}^{(1)}(-\omega) \right] \right\} \quad (24)$$

2) $\beta = 1$:

$$D_{ll}^{IB}(-2\omega; \omega, \omega) = \frac{i\sqrt{\pi}}{\gamma_{lg}} \left\{ \frac{1}{\omega} \left[W_l(-2\omega) - W_l(-\omega) + W_l^*(\omega) - W_l^*(2\omega) \right] + \frac{1}{2(\omega + i\Gamma_{lg})} \left[W_l(-\omega) - W_l^*(\omega) \right] \right\} \quad (25)$$

$$D_{lm}^{IB}(-2\omega; \omega, \omega) = \frac{-\pi}{\gamma_{lg}\gamma_{mg}} \left\{ W_l(-2\omega)W_m(-\omega) + W_l^*(\omega) \left[W_m^*(2\omega) + W_m(-\omega) \right] \right\} \quad (26)$$

B. Linear Electrooptic Effect

1) $\beta \leq 1$:

$$D_{ll}^{IB}(-\omega; \omega, 0) = \frac{i\sqrt{\pi}}{\gamma_{lg}} \left\{ \frac{-1}{\gamma_{lg}} \left[W_{\beta_l}^{(2)*}(\omega) + W_{\beta_l}^{(2)}(-\omega) \right] + \frac{2(\omega + i\Gamma_{lg})}{\omega(\omega + 2i\Gamma_{lg})} \left[W_{\beta_l}^{(1)}(-\omega) - W_{\beta_l}^{(1)*}(\omega) \right] + \frac{2i\Gamma_{lg}}{(\omega + 2i\Gamma_{lg})} \left[W_{\beta_l}^{(1)*}(0) - W_{\beta_l}^{(1)}(0) \right] \right\} \quad (27)$$

$$D_{lm}^{IB}(-\omega; \omega, 0) = \frac{-\pi}{\gamma_{lg}\gamma_{mg}} \left\{ W_{\beta_l}^{(1)}(-\omega) \left[W_{\beta_m}^{(1)}(0) + W_{\beta_m}^{(1)}(-\omega) \right] + W_{\beta_l}^{(1)*}(\omega) \left[W_{\beta_m}^{(1)*}(\omega) + W_{\beta_m}^{(1)}(0) \right] + W_{\beta_l}^{(1)*}(0) \left[W_{\beta_m}^{(1)*}(\omega) - W_{\beta_m}^{(1)}(-\omega) \right] \right\} \quad (28)$$

2) $\beta = 1$:

$$D_{ll}^{IB}(-\omega; \omega, 0) = \frac{i\sqrt{\pi}}{\gamma_{lg}} \left\{ \frac{2}{\gamma_{lg}^2} \left[(\Omega_{lg}^* + \omega)W_l^*(\omega) + (\Omega_{lg} - \omega)W_l(-\omega) \right] + \frac{4i}{\gamma_{lg}\sqrt{\pi}} + \frac{2(\omega + i\Gamma_{lg})}{\omega(\omega + 2i\Gamma_{lg})} \left[W_l(-\omega) - W_l^*(\omega) \right] + \frac{2i\Gamma_{lg}}{(\omega + 2i\Gamma_{lg})} \left[W_l^*(0) - W_l(0) \right] \right\} \quad (29)$$

$$D_{lm}^{IB}(-\omega; \omega, 0) = \frac{-\pi}{\gamma_{lg}\gamma_{mg}} \left\{ W_l(-\omega) \left[W_m(0) + W_m(-\omega) \right] + W_l^*(\omega) \left[W_m^*(\omega) + W_m(0) \right] + W_l^*(0) \left[W_m^*(\omega) - W_m(-\omega) \right] \right\} \quad (30)$$

C. Sum and Difference Frequency Generation

1) $\beta \leq 1$:

$$\begin{aligned}
D_{ll}^{IB}(-(\omega_1 + \omega_2); \omega_1, \omega_2) &= \frac{i\sqrt{\pi}}{\gamma_{lg}} \left\{ \frac{1}{\omega_1 + \omega_2 + 2i\Gamma_{lg}} \left[W_{\beta_l}^{(1)}(-\omega_1) - W_{\beta_l}^{(1)*}(\omega_2) + W_{\beta_l}^{(1)}(-\omega_2) - W_{\beta_l}^{(1)*}(\omega_1) \right] \right. \\
&+ \frac{1}{\omega_1} \left[W_{\beta_l}^{(1)}(-\omega_1 - \omega_2) - W_{\beta_l}^{(1)}(-\omega_2) + W_{\beta_l}^{(1)*}(\omega_1 + \omega_2) - W_{\beta_l}^{(1)*}(\omega_2) \right] \\
&\left. + \frac{1}{\omega_2} \left[W_{\beta_l}^{(1)}(-\omega_1 - \omega_2) - W_{\beta_l}^{(1)}(-\omega_1) + W_{\beta_l}^{(1)*}(\omega_1 + \omega_2) - W_{\beta_l}^{(1)*}(\omega_1) \right] \right\} \quad (31)
\end{aligned}$$

$$\begin{aligned}
D_{lm}^{IB}(-(\omega_1 + \omega_2); \omega_1, \omega_2) &= \frac{-\pi}{\gamma_{lg}\gamma_{mg}} \left\{ W_{\beta_l}^{(1)}(-\omega_1 - \omega_2) \left[W_{\beta_m}^{(1)}(-\omega_1) + W_{\beta_m}^{(1)}(-\omega_2) \right] \right. \\
&\left. + W_{\beta_l}^{(1)*}(\omega_2) \left[W_{\beta_m}^{(1)*}(\omega_1 + \omega_2) + W_{\beta_m}^{(1)}(-\omega_1) \right] + W_{\beta_l}^{(1)*}(\omega_1) \left[W_{\beta_m}^{(1)*}(\omega_1 + \omega_2) + W_{\beta_m}^{(1)}(-\omega_2) \right] \right\} \quad (32)
\end{aligned}$$

2) $\beta = 1$:

$$\begin{aligned}
D_{ll}^{IB}(-(\omega_1 + \omega_2); \omega_1, \omega_2) &= \frac{i\sqrt{\pi}}{\gamma_{lg}} \left\{ \frac{1}{\omega_1} \left[W_l(-\omega_1 - \omega_2) - W_l(-\omega_2) + W_l^*(\omega_1 + \omega_2) - W_l^*(\omega_2) \right] \right. \\
&+ \frac{1}{\omega_2} \left[W_l(-\omega_1 - \omega_2) - W_l(-\omega_1) + W_l^*(\omega_1 + \omega_2) - W_l^*(\omega_1) \right] \\
&\left. + \frac{1}{\omega_1 + \omega_2 + 2i\Gamma_{lg}} \left[W_l(-\omega_1) - W_l^*(\omega_2) + W_l(-\omega_2) - W_l^*(\omega_1) \right] \right\} \quad (33)
\end{aligned}$$

$$\begin{aligned}
D_{lm}^{IB}(-(\omega_1 + \omega_2); \omega_1, \omega_2) &= \frac{-\pi}{\gamma_{lg}\gamma_{mg}} \left\{ W_l(-\omega_1 - \omega_2) \left[W_m(-\omega_1) + W_m(-\omega_2) \right] \right. \\
&\left. + W_l^*(\omega_2) \left[W_m^*(\omega_1 + \omega_2) + W_m(-\omega_1) \right] + W_l^*(\omega_1) \left[W_m^*(\omega_1 + \omega_2) + W_m(-\omega_2) \right] \right\} \quad (34)
\end{aligned}$$